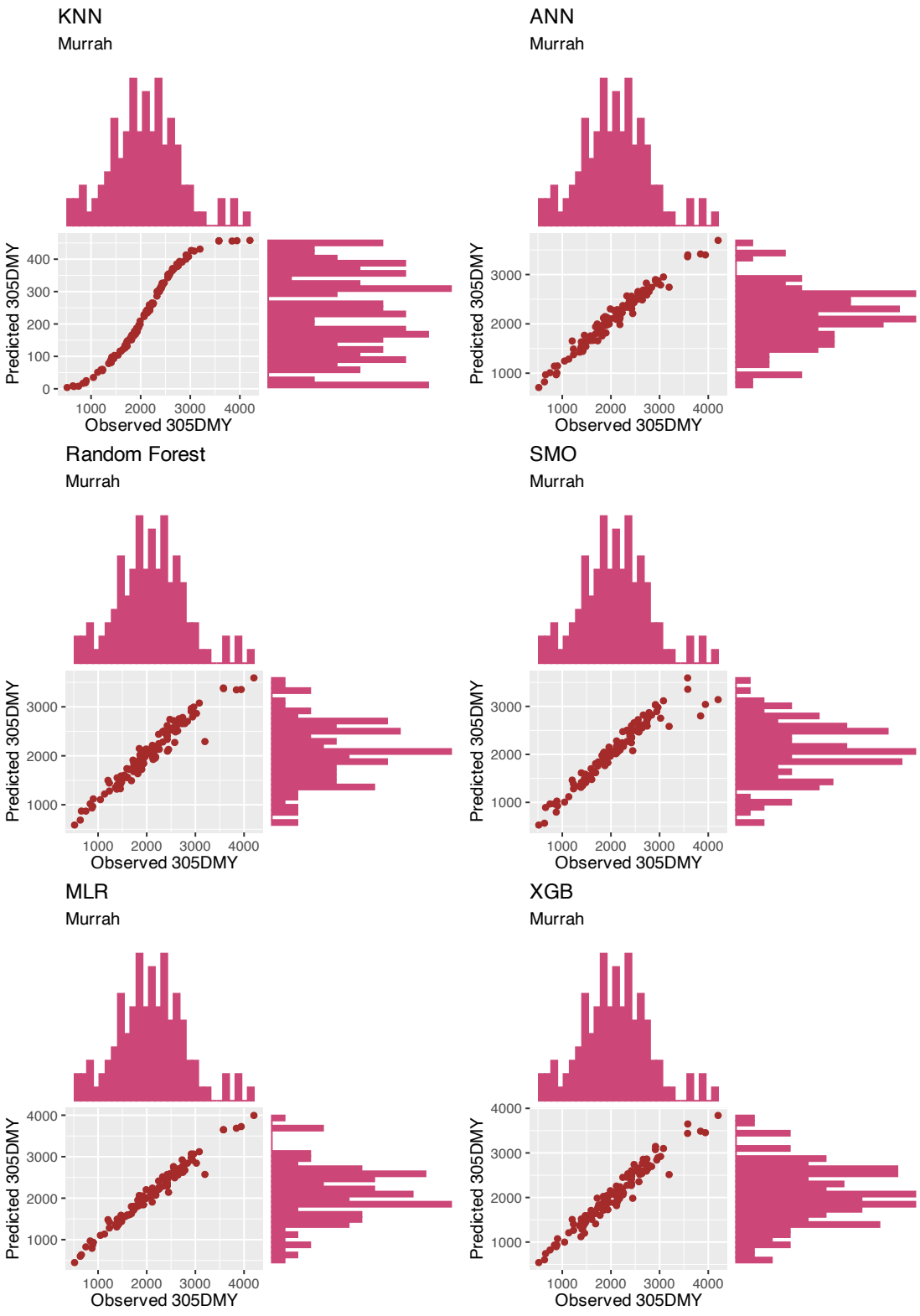

Figure 4.1: Scatter plots with histogram of predicted vs observed values of 305DMY using STDMY in Murrah buffaloes - (a) KNN, (b) ANN, (c) RF, (d) SMOreg, (e) MLR, (f) XGB

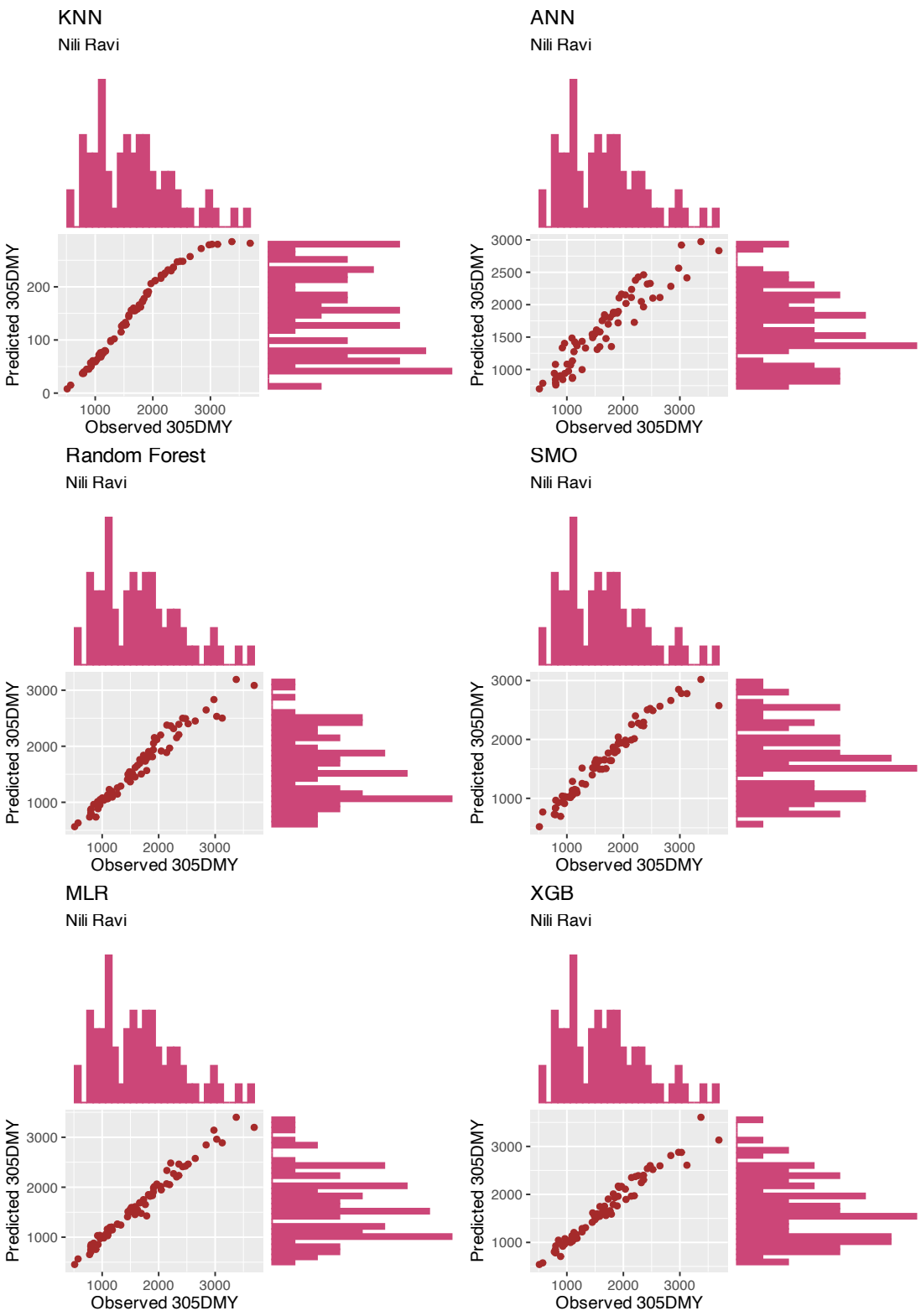

Figure 4.2: Scatter plots with histogram of predicted vs observed values of 305DMY using STDMY in Nili Ravi buffaloes - (a) KNN, (b) ANN, (c) RF, (d) SMOreg, (e) MLR, (f) XGB

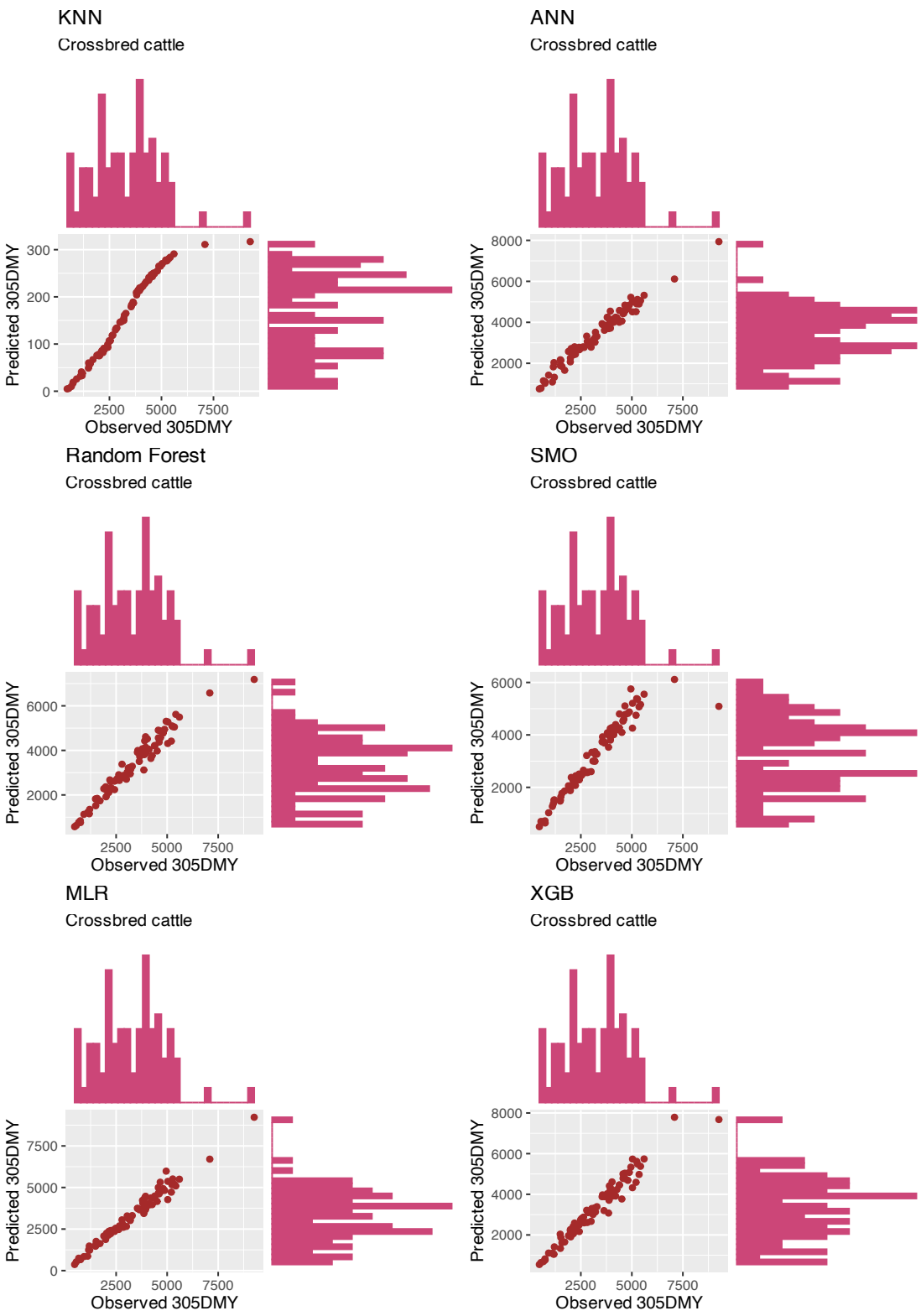

Figure 4.3: Scatter plots with histogram of predicted vs observed values of 305DMY using STDMY in crossbred cattle - (a) KNN, (b) ANN, (c) RF, (d) SMOreg, (e) MLR, (f) XGB

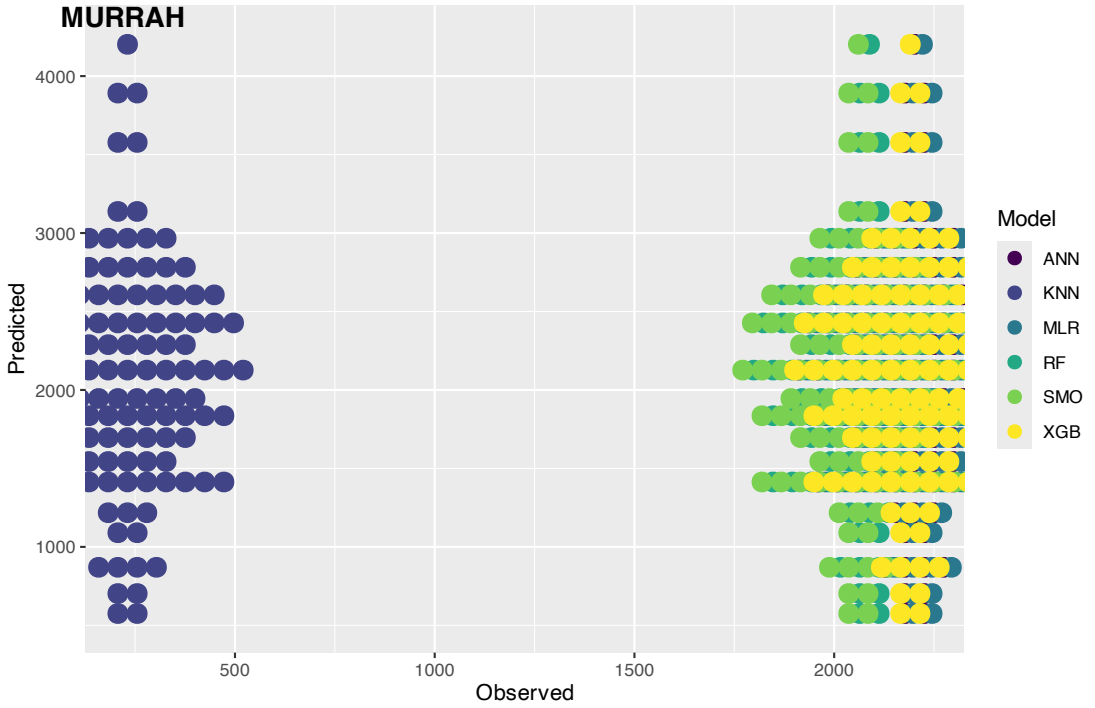

Figure 4.4: Observed and predicted 305DMY in Murrah buffaloes using STDMY

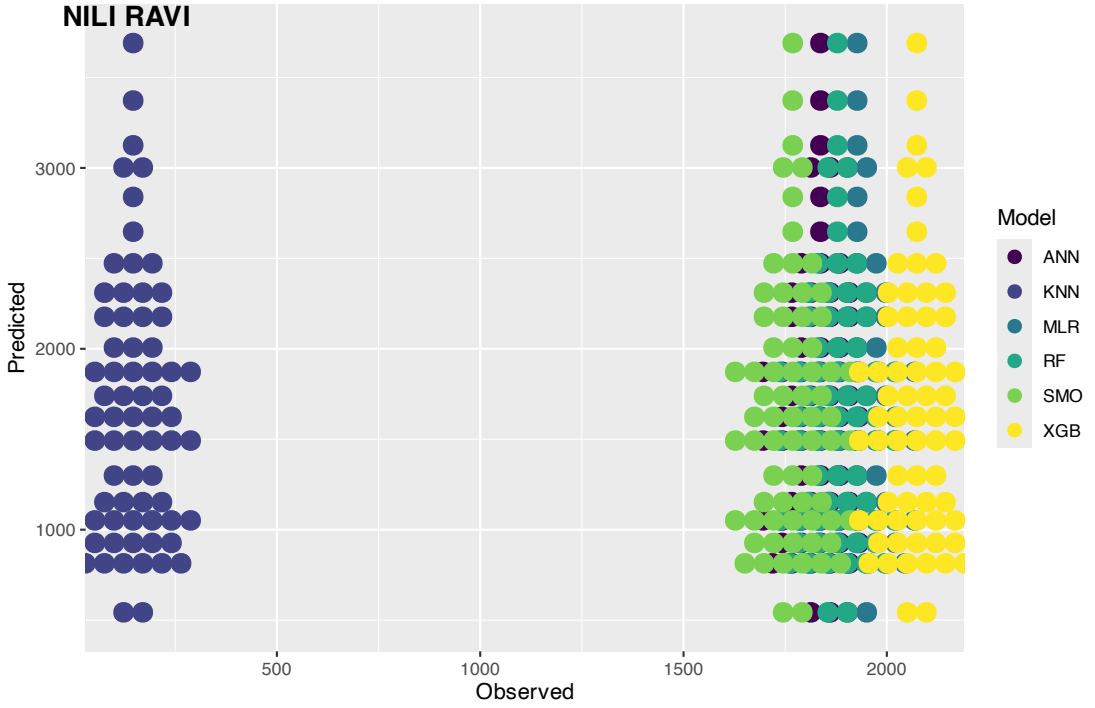

Figure 4.5: Observed and predicted 305DMY in Nili Ravi buffaloes using STDMY

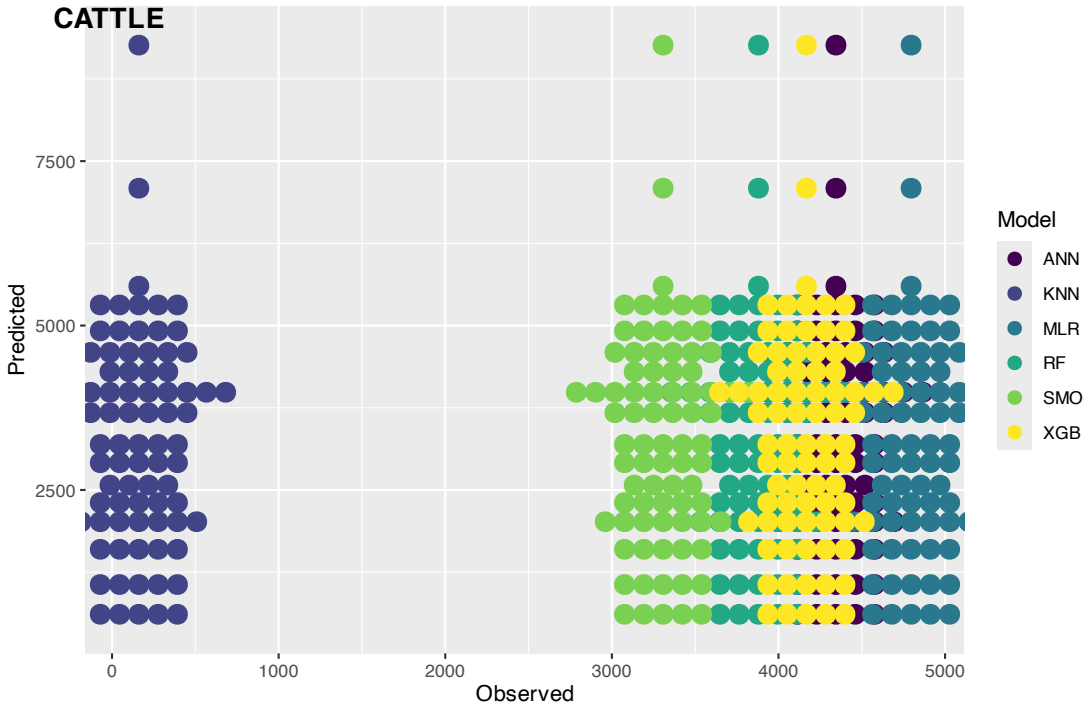

Figure 4.6: Observed and predicted 305DMY in crossbred cattle using STDMY

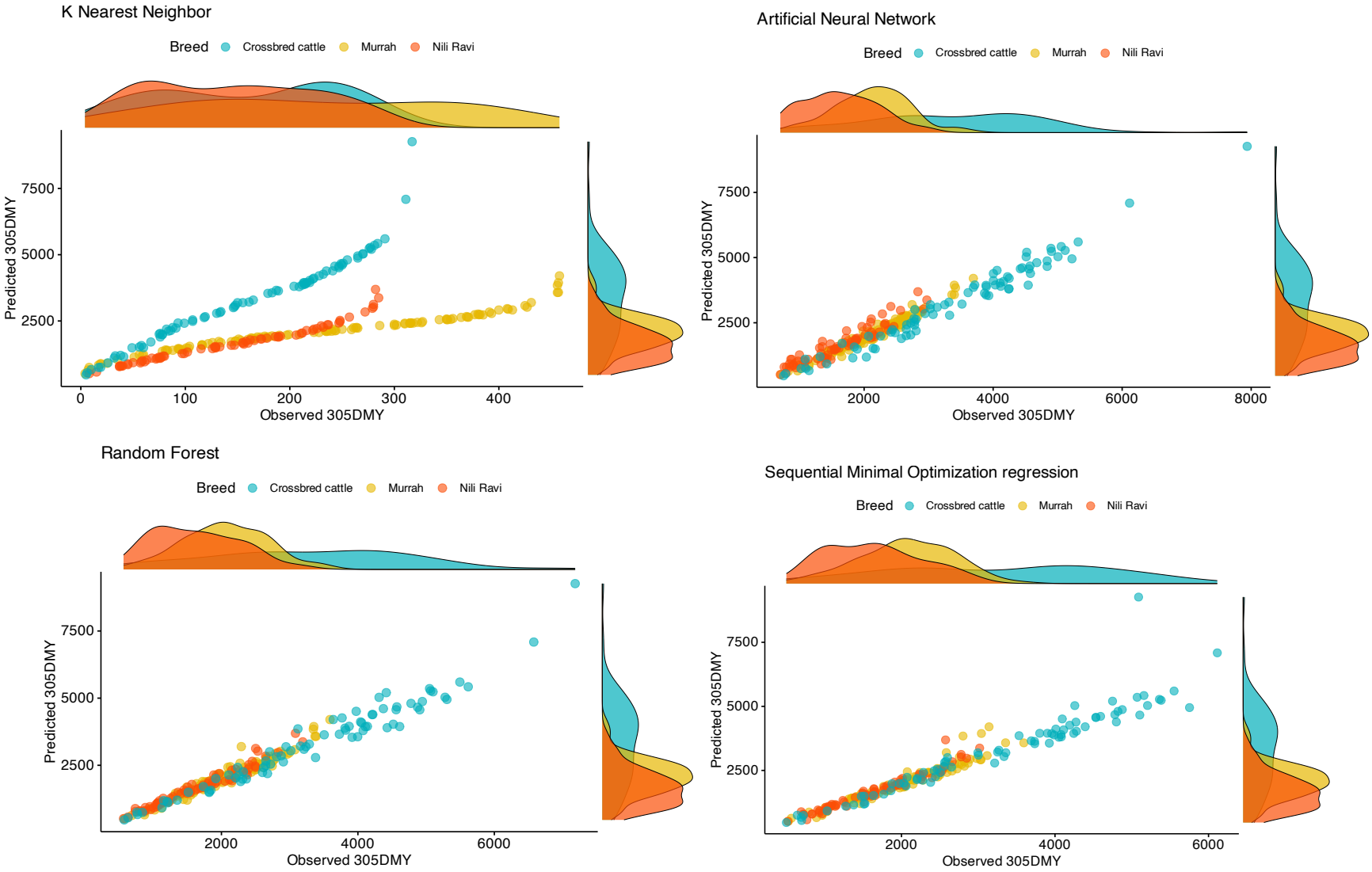

Figure 4.7: Comparative analysis of individual Model Efficiency: (a) KNN, (b) ANN, (c) RF, (d) SMOreg

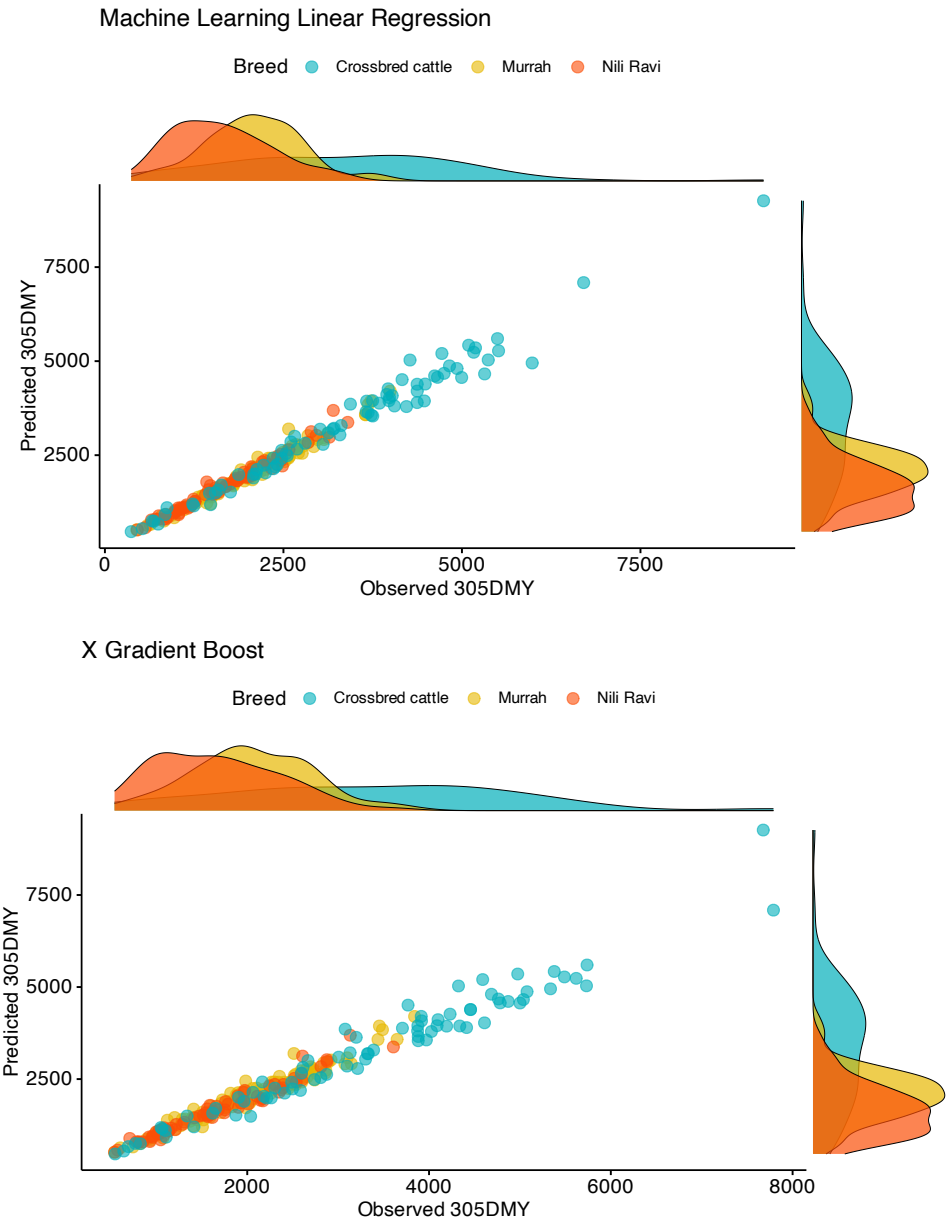

Figure 4.7: Comparative analysis of individual Model Efficiency: (e) MLR, (f) XGB

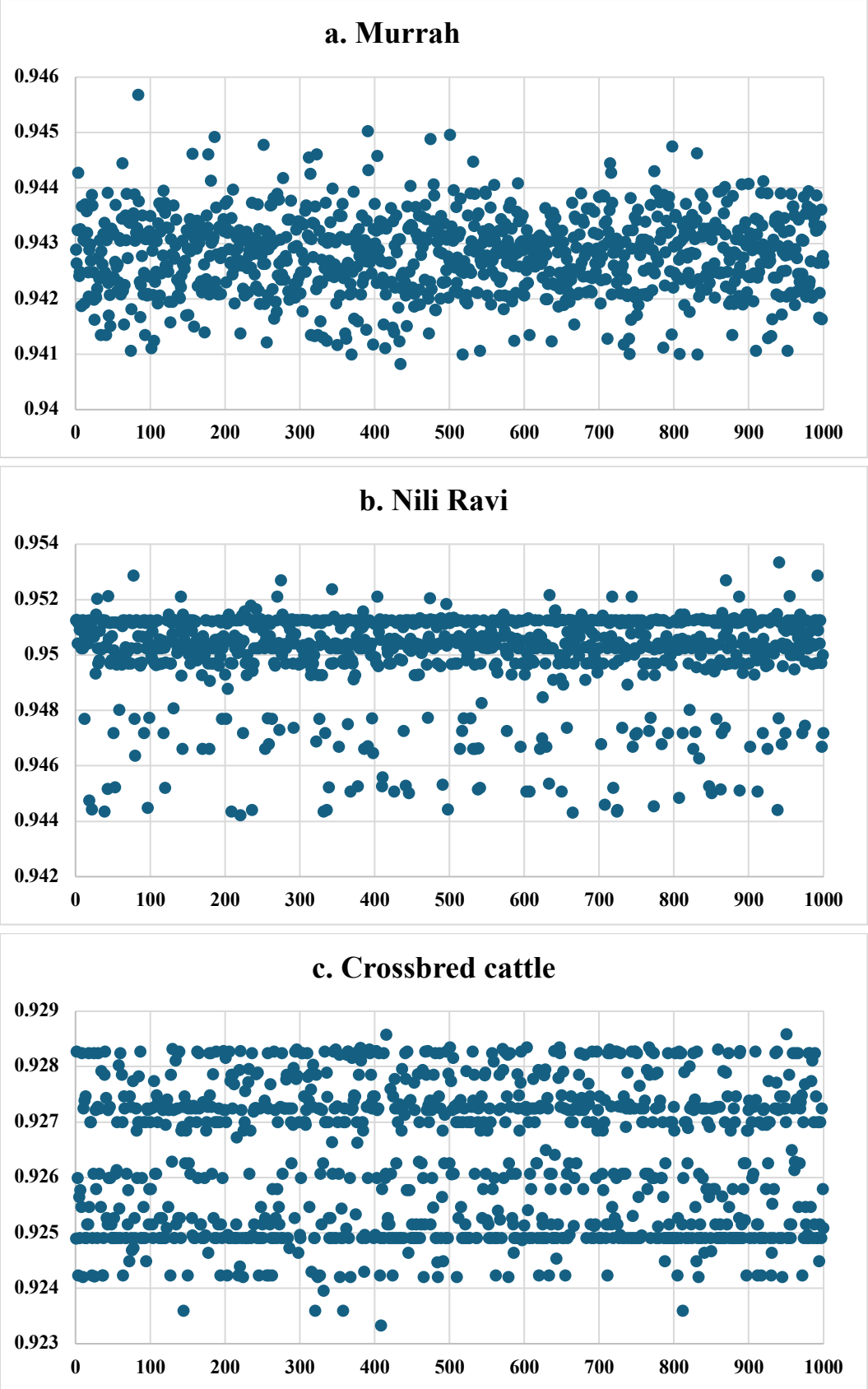

Figure 4.8: Variability in Adjusted R^2 for K Nearest Neighbor using the 1000 RTDMY sets

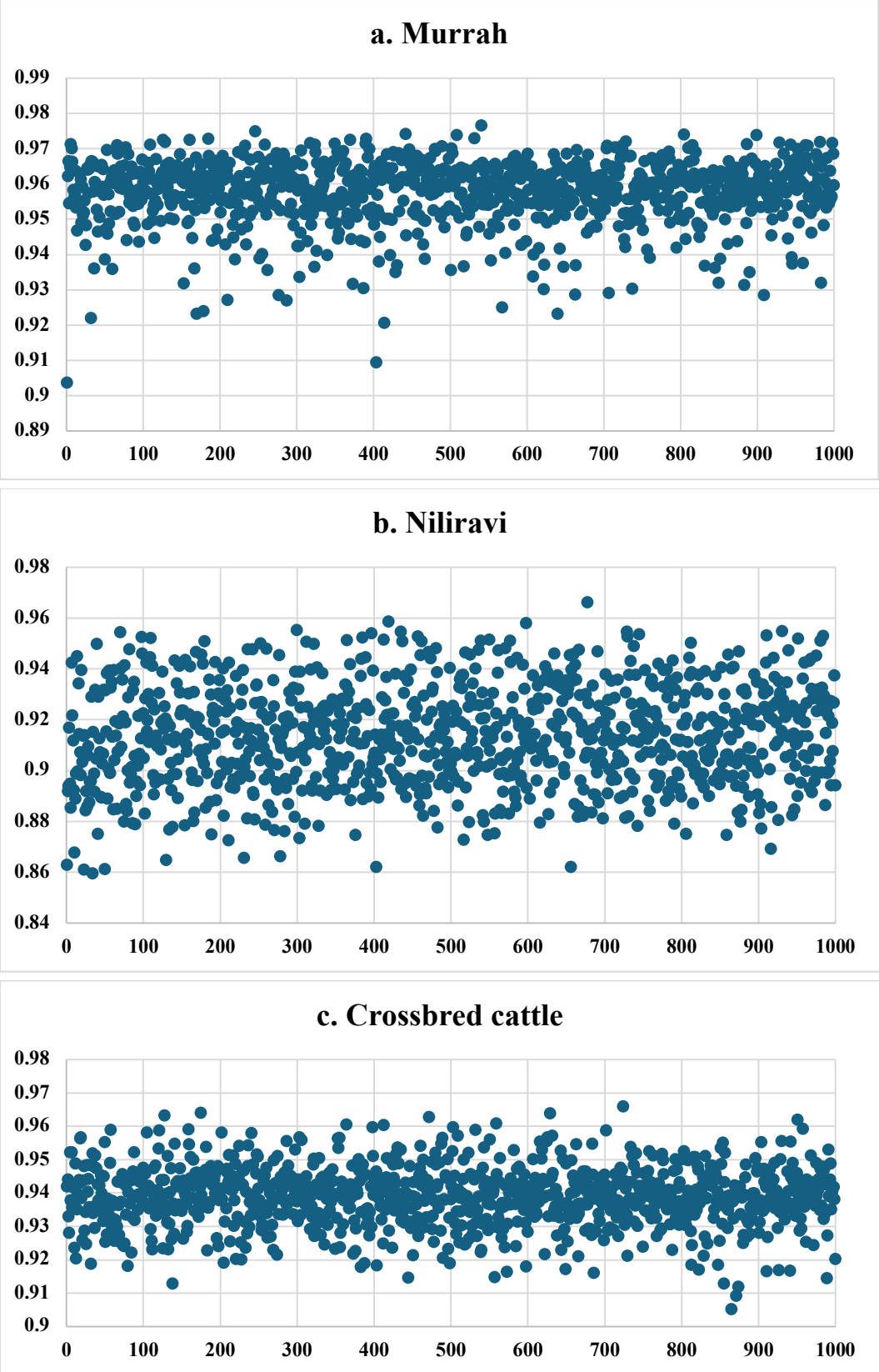

Figure 4.9: Variability in Adjusted R^2 for Artificial Neural Network using the 1000 RTDMY sets

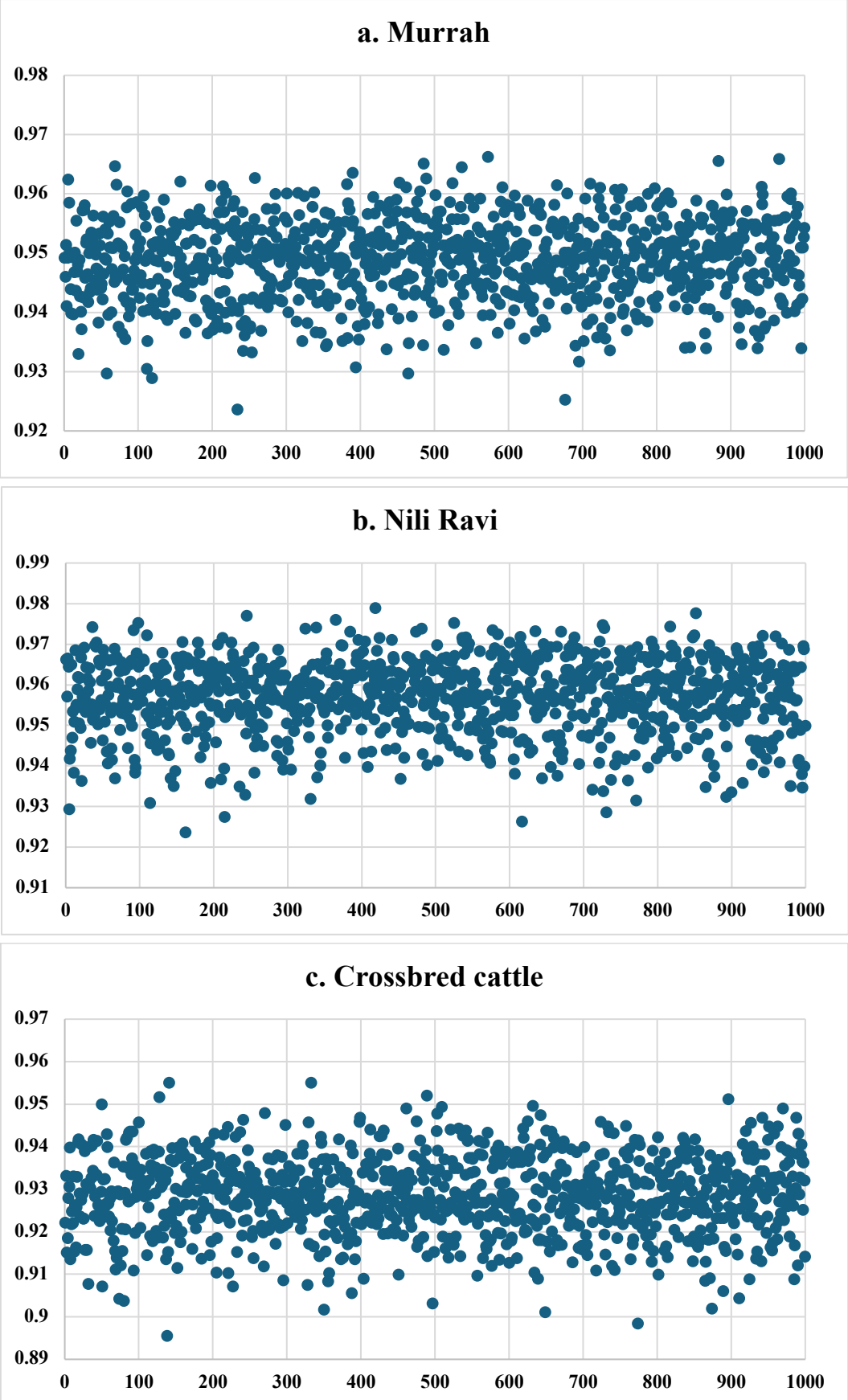

Figure 4.10: Variability in Adjusted R^2 for Random Forest using the 1000 RTDMY sets

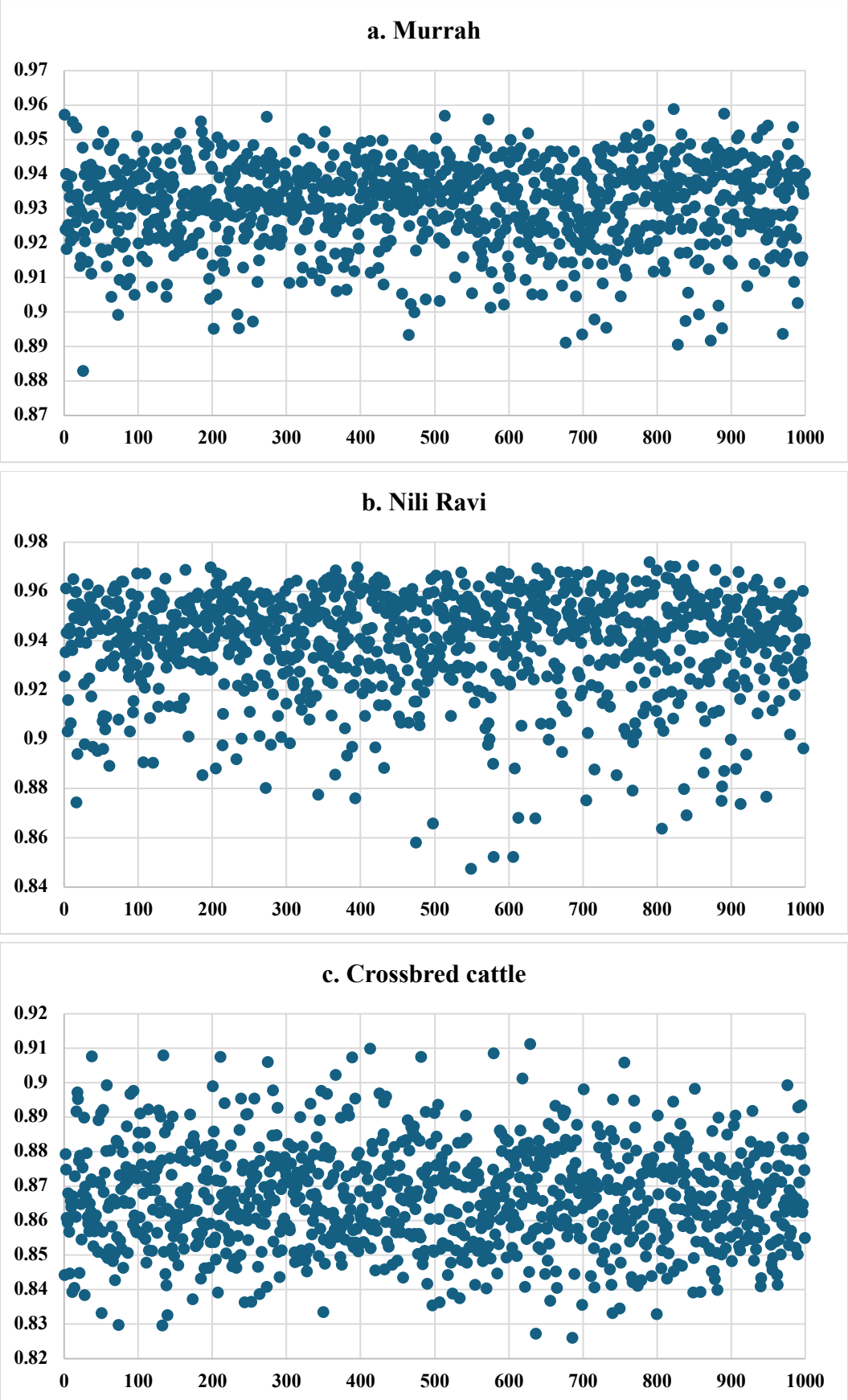

Figure 4.11: Variability in Adjusted R^2 for Sequential Minimal Optimization regression using the 1000 RTDMY sets

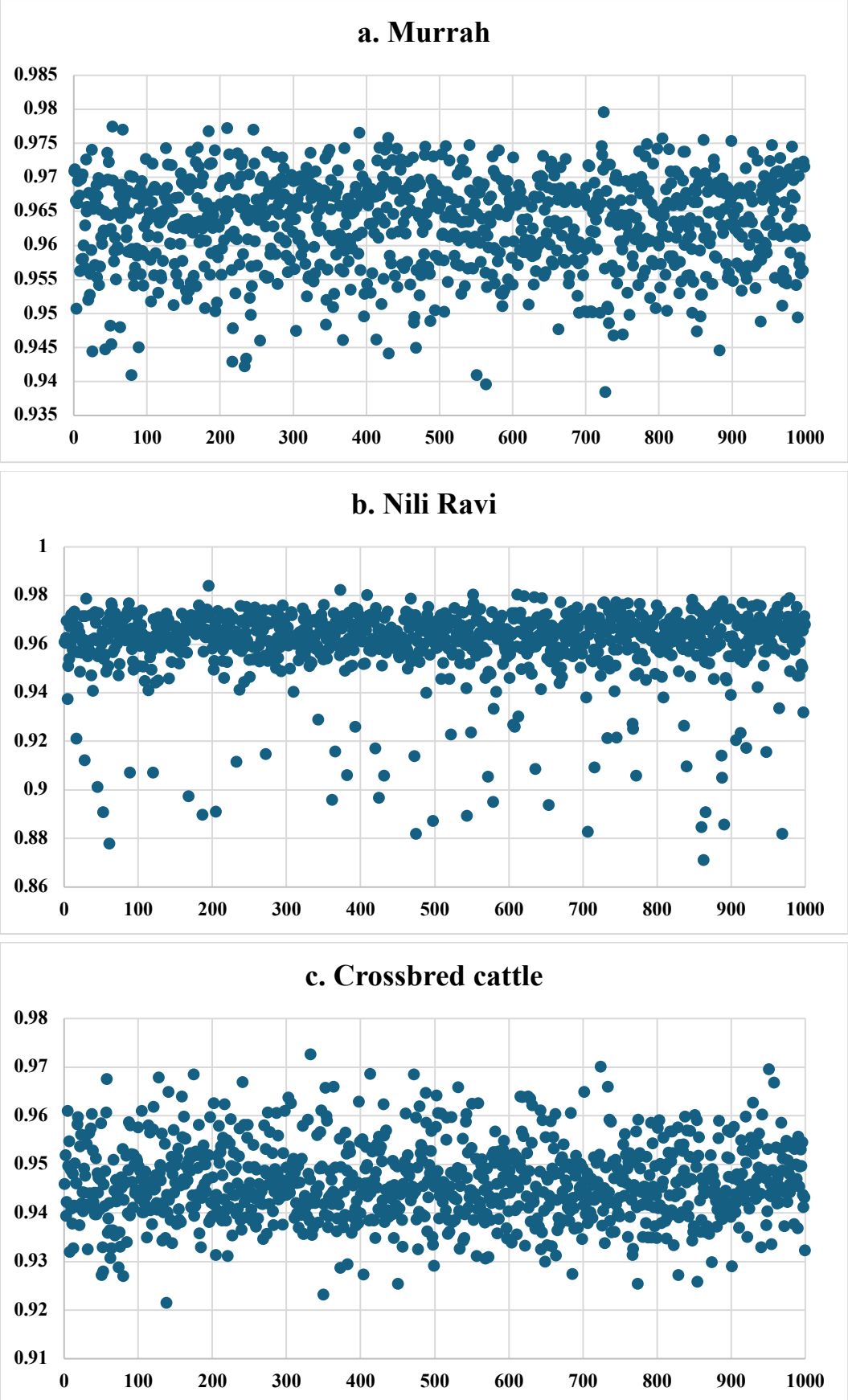

Figure 4.12: Variability in Adjusted R^2 for Machine learning linear regression using the 1000 RTDMY sets

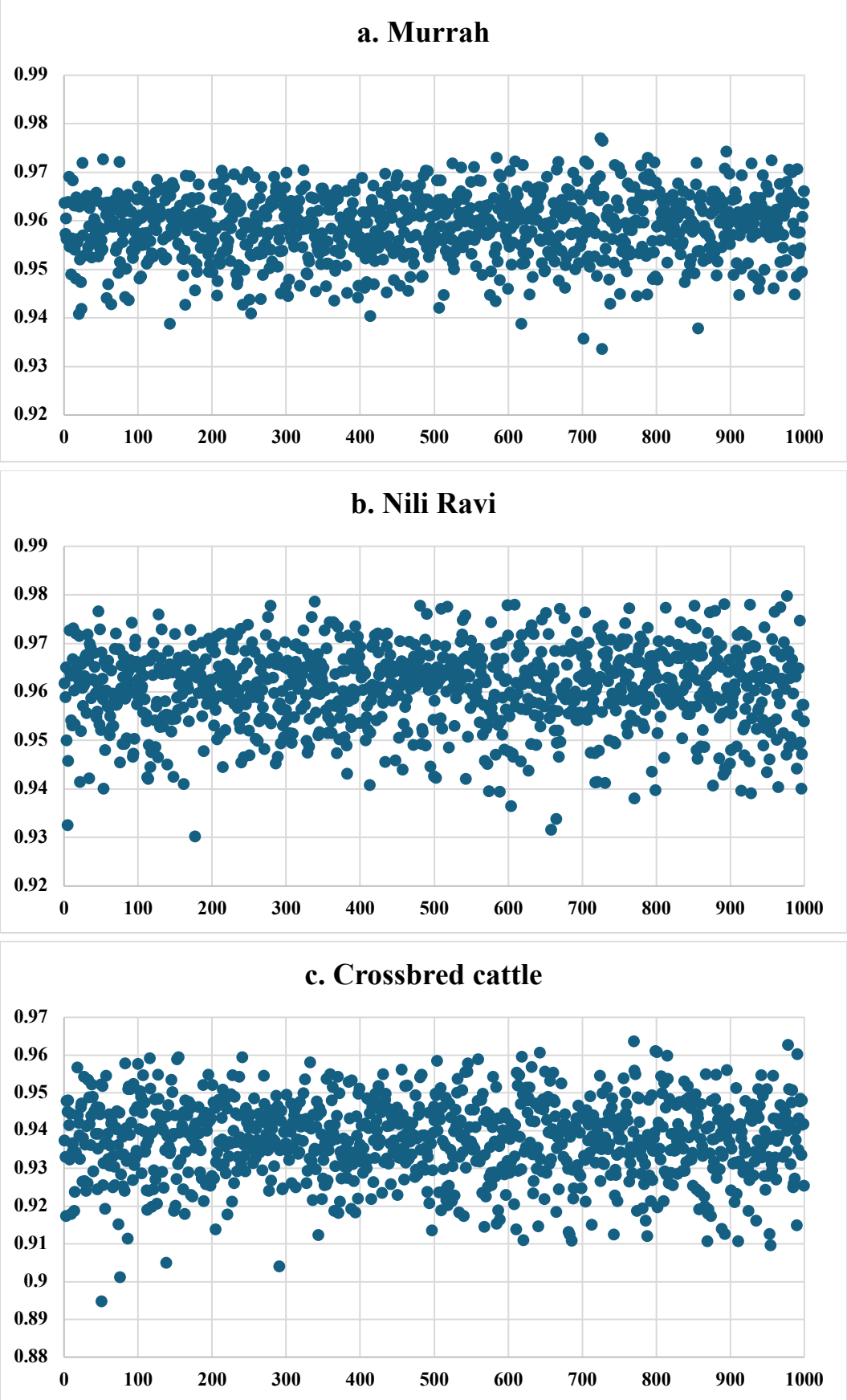

Figure 4.13: Variability in Adjusted R^2 for xEtreme Gradient Boost using the 1000 RTDMY sets

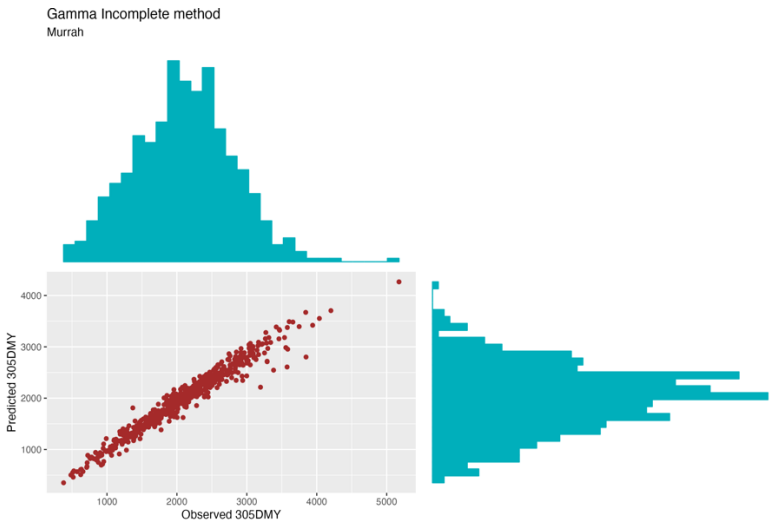

Figure 4.14: Scatter plots with marginal histogram of predicted vs observed values of 305DMY using STDMY in Murrah buffaloes - Wood's Lactation curve model

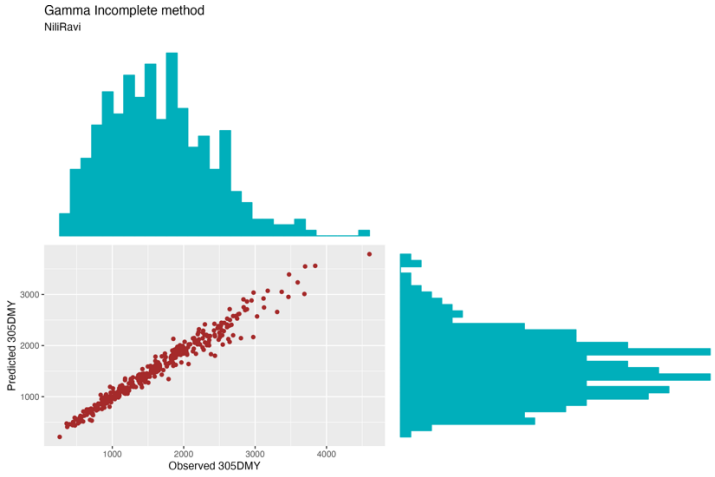

Figure 4.15: Scatter plots with marginal histogram of predicted vs observed values of 305DMY using STDMY in Nili Ravi buffaloes - Wood's Lactation curve model

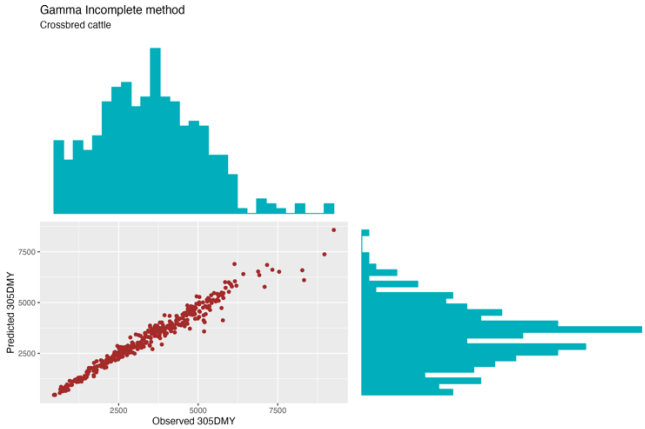

Figure 4.16: Scatter plots with marginal histogram of predicted vs observed values of 305DMY using STDMY in crossbred cattle - Wood's Lactation curve model

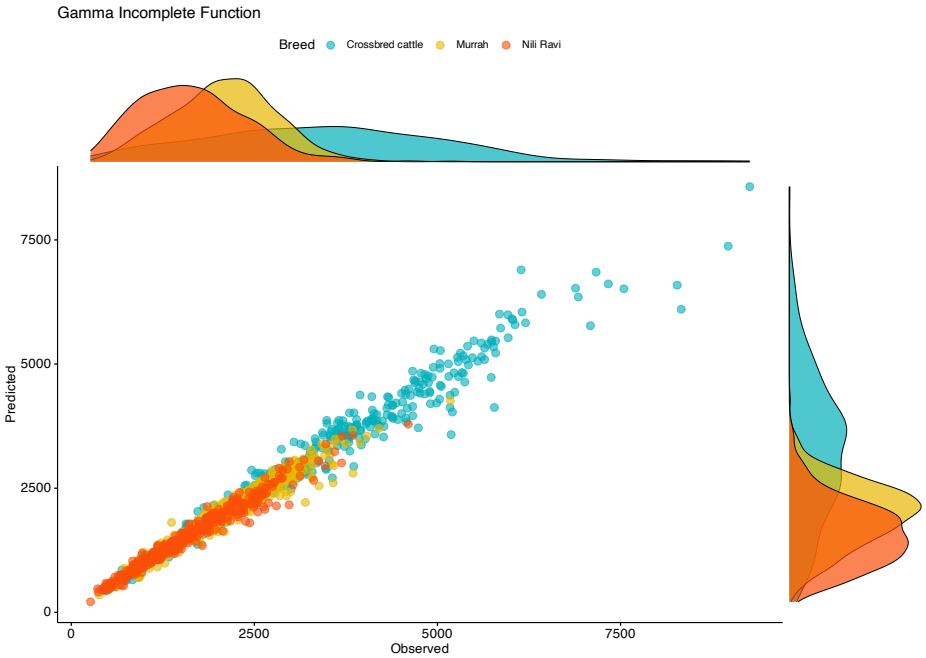

Figure 4.17: Grouped Scatter plot with marginal density plots of predicted vs observed 305DMY in three different breeds - Gamma incomplete function (Wood's Lactation curve model)

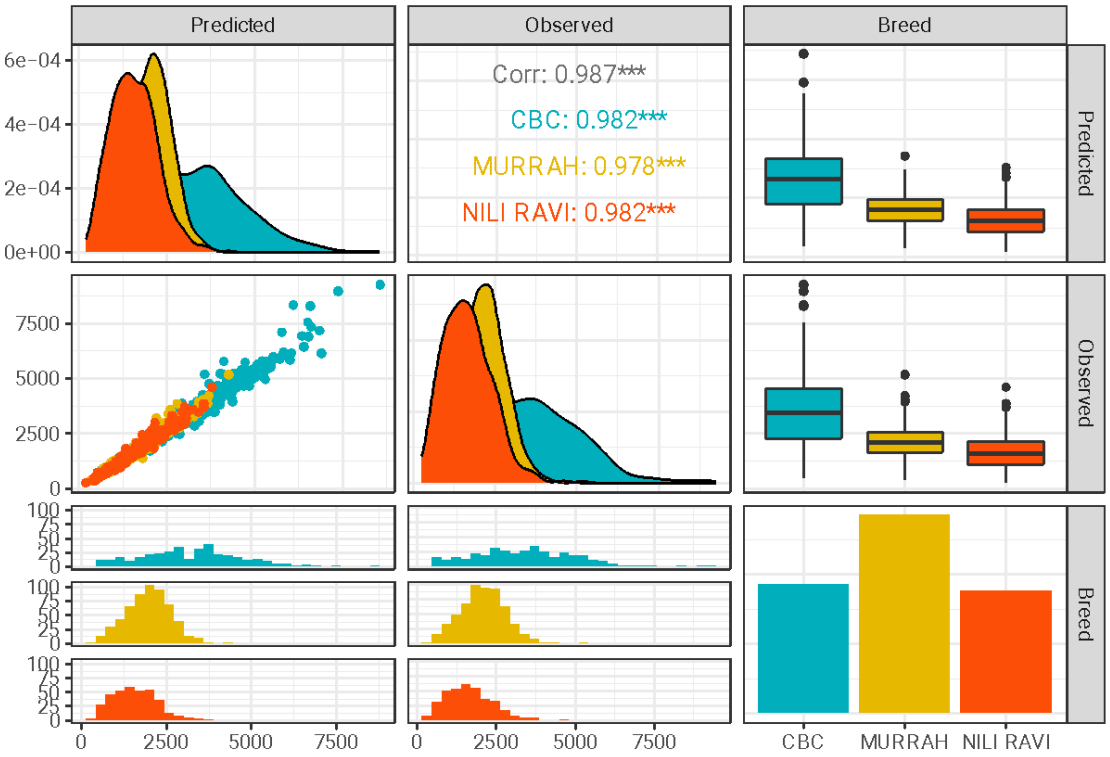

Figure 4.18: Scatter plot matrix of Wood's lactation curve model of predicted vs observed 305DMY

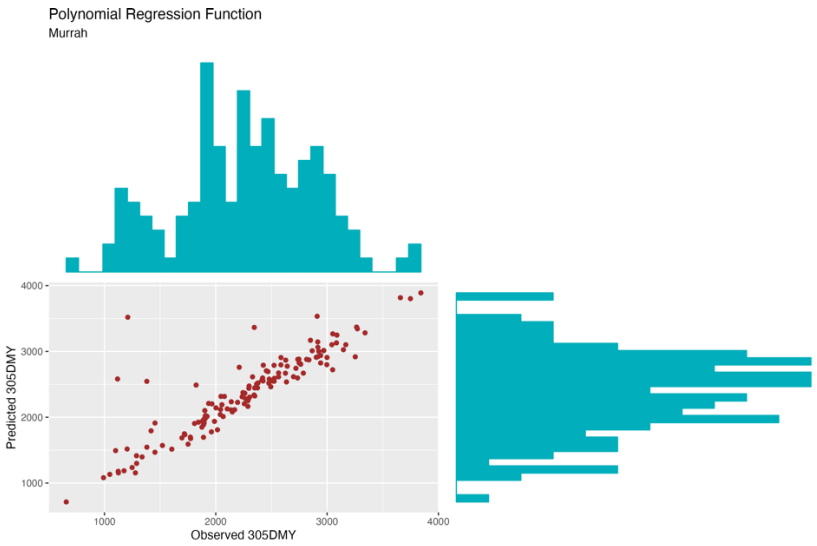

Figure 4.19: Scatter plots with marginal histogram of predicted vs observed values of 305DMY using STDMY in Murrah buffaloes - Polynomial Regression function

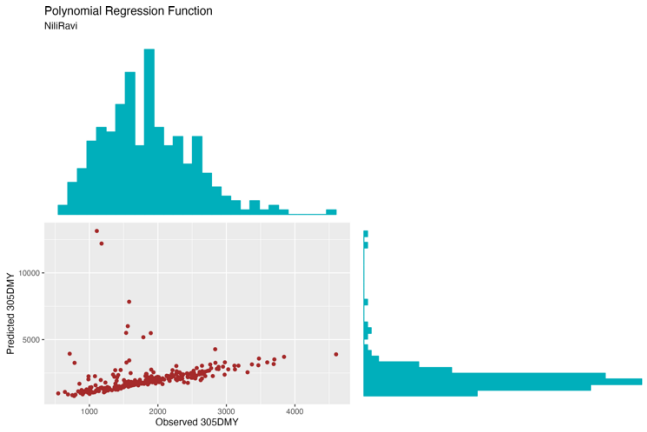

Figure 4.20: Scatter plots with marginal histogram of predicted vs observed values of 305DMY using STDMY in Nili Ravi buffaloes - Polynomial Regression function

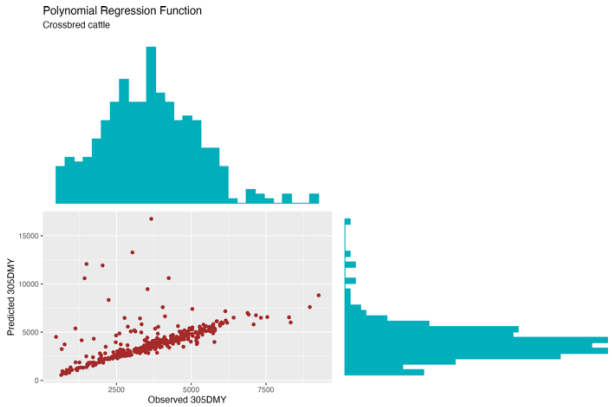

Figure 4.21: Scatter plots with marginal histogram of predicted vs observed values of 305DMY using STDMY in crossbred cattle - Polynomial Regression function

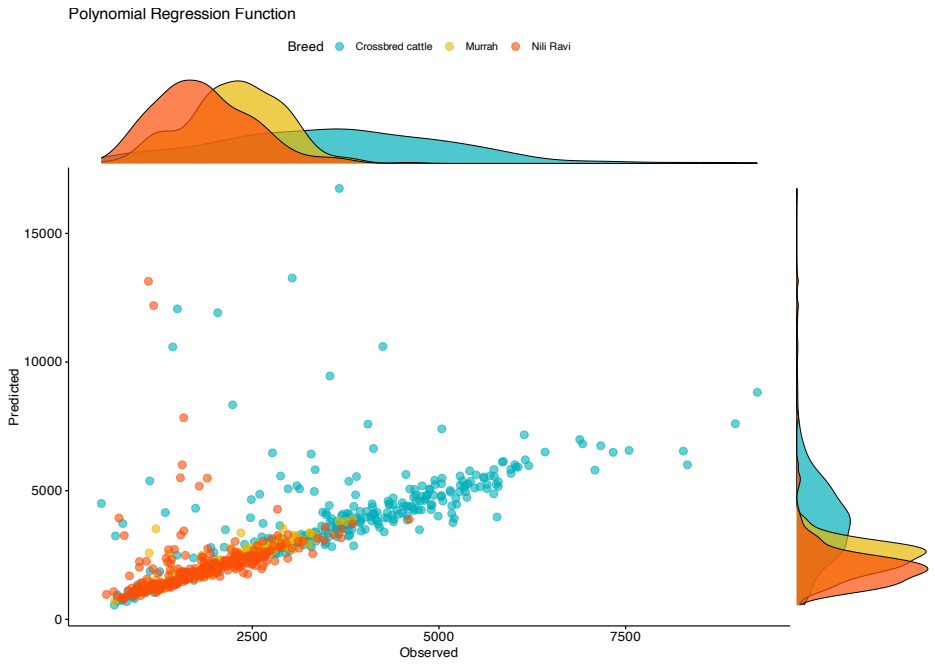

Figure 4.22: Grouped Scatter plot with marginal density plots of predicted vs observed 305DMY in three different breeds - Polynomial Regression Function

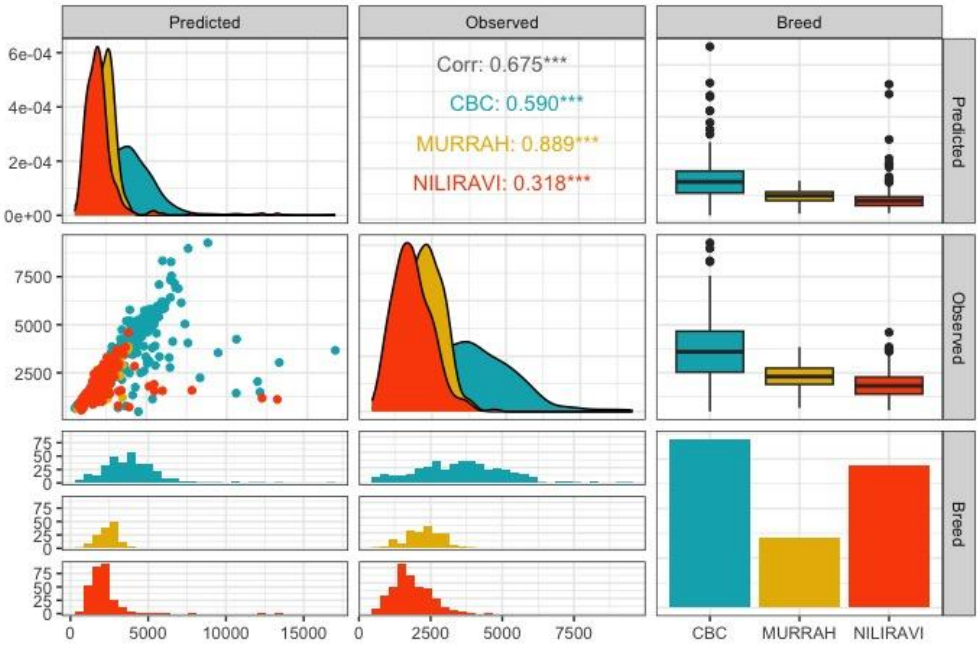

Figure 4.23: Scatter plot matrix of Polynomial Regression function of predicted vs observed 305DMY

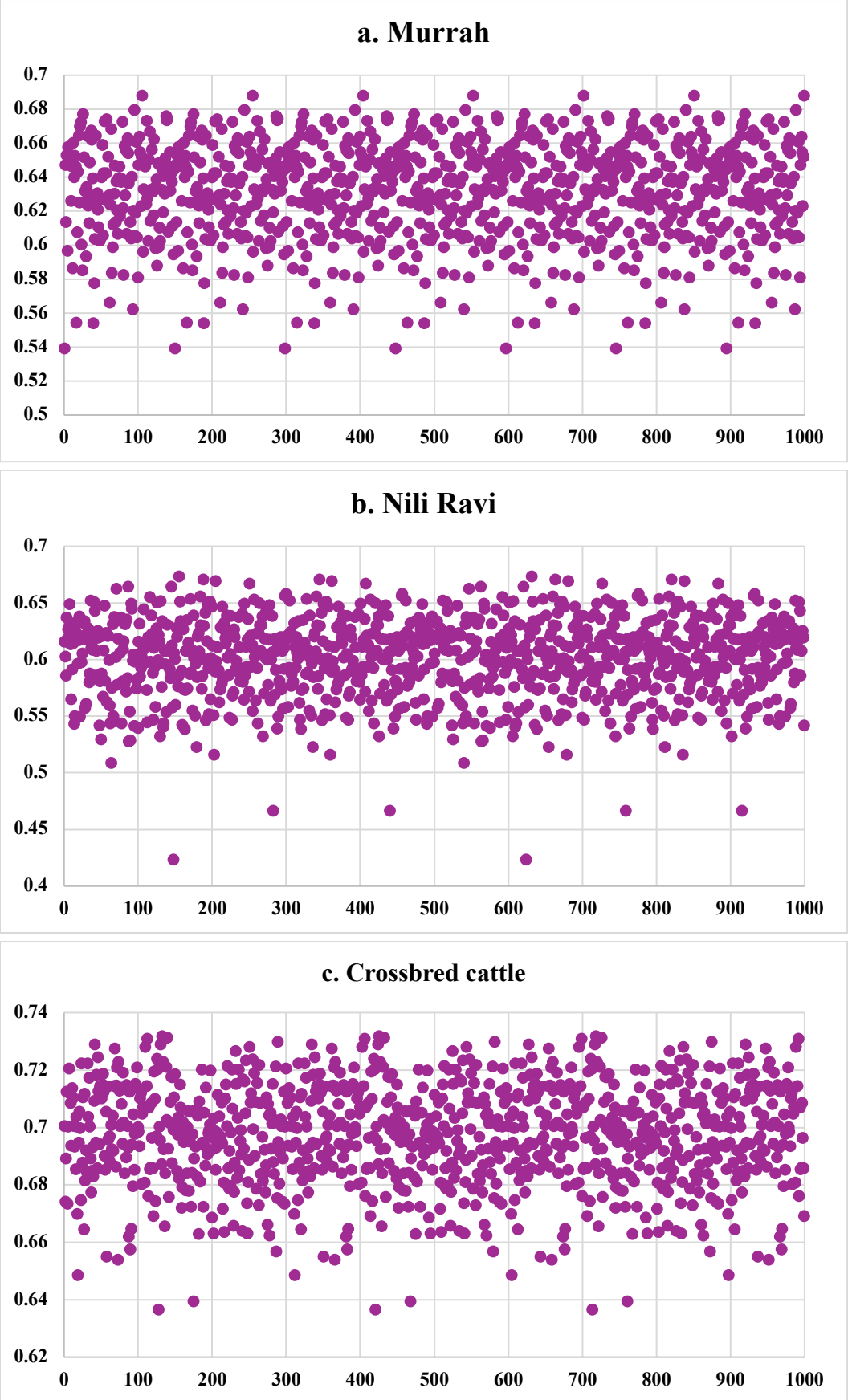

Figure 4.24: Variability in Adjusted R^2 for Wood's lactation curve model using the 1000 RTDMY sets

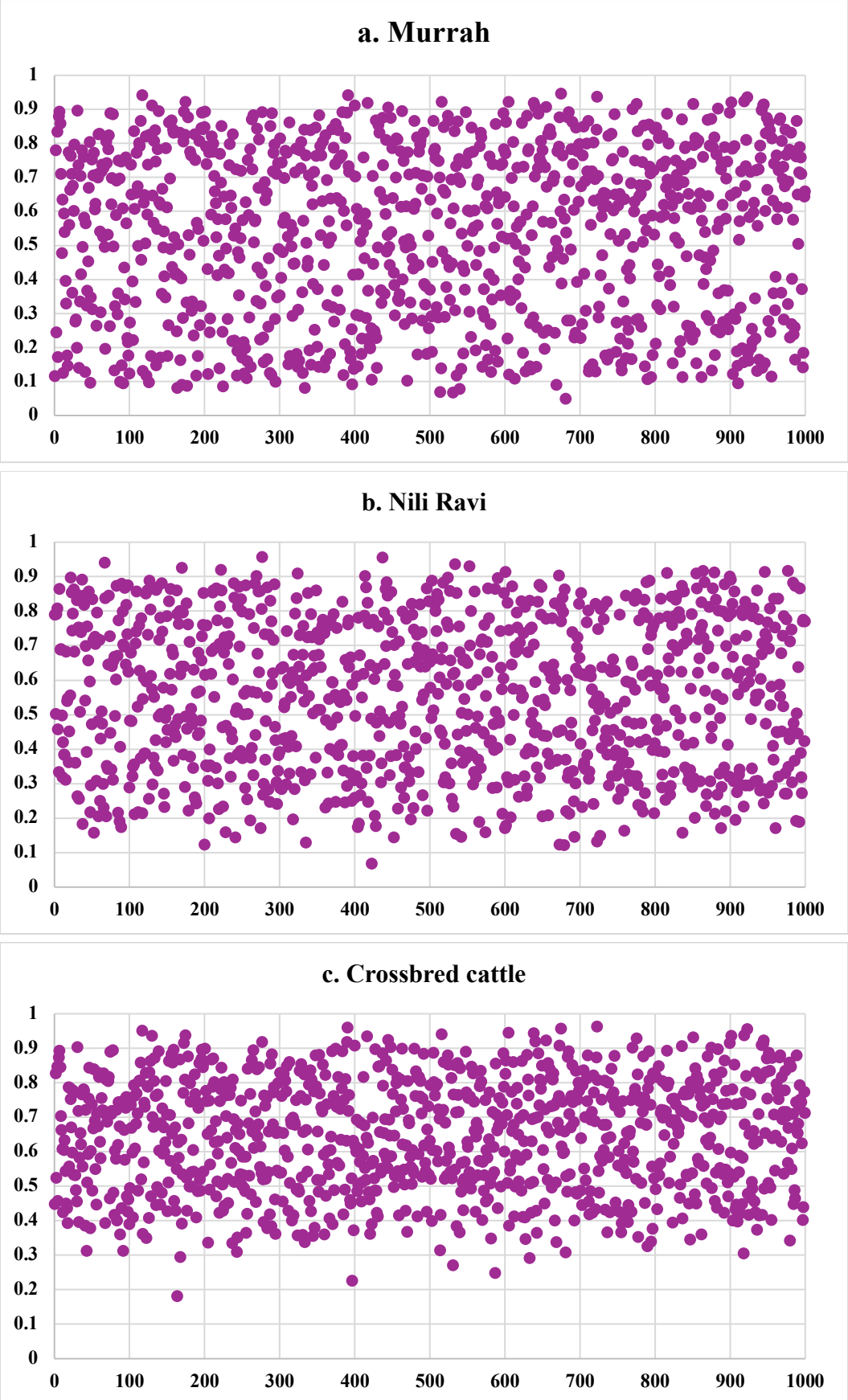

Figure 4.25: Variability in Adjusted R^2 for PRF model using the 1000 RTDMY sets

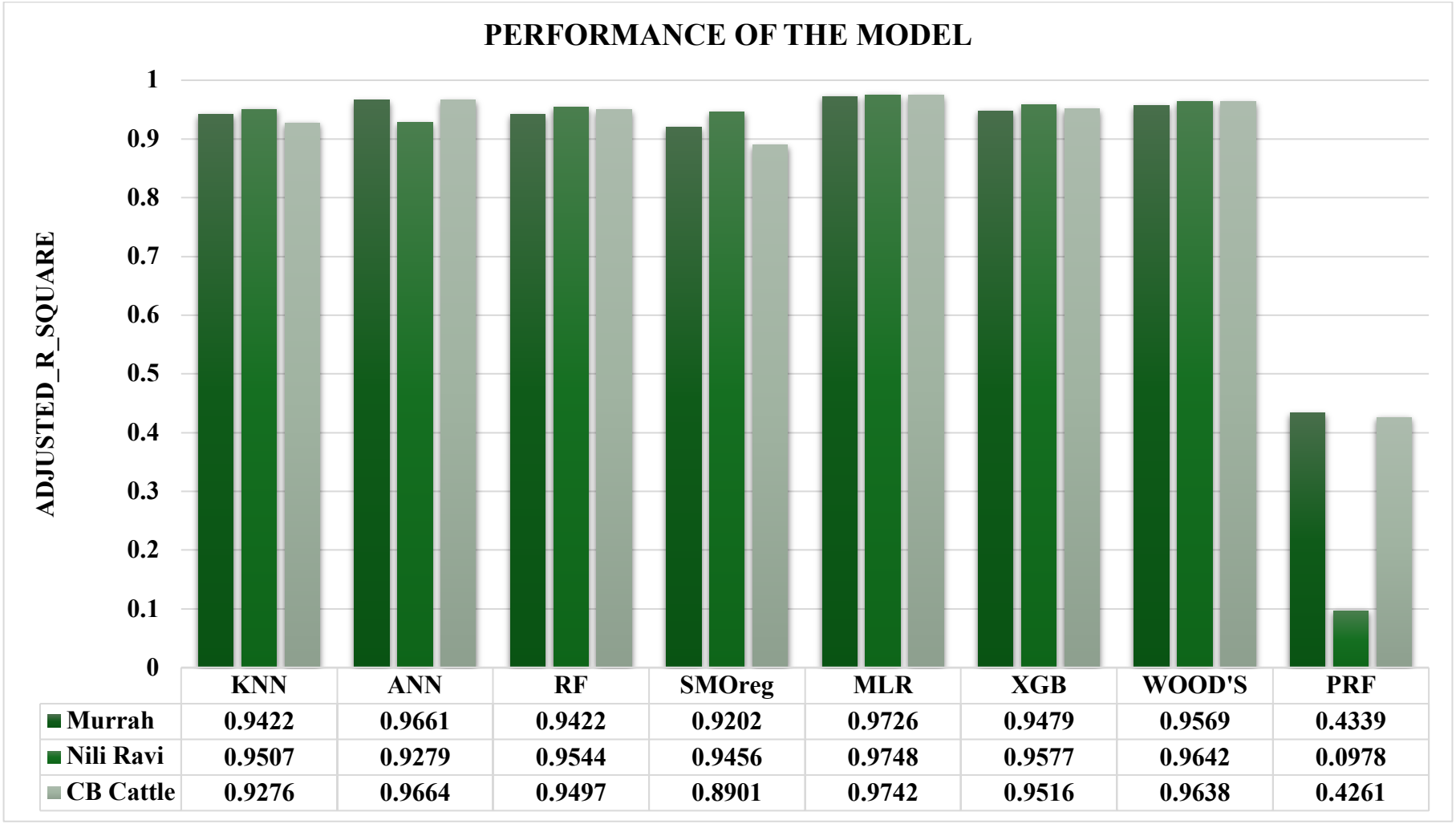

	KNN	ANN	RF	SMOreg	MLR	XGB	WOOD'S	PRF
Murrah	0.9422	0.9661	0.9422	0.9202	0.9726	0.9479	0.9569	0.4339
Nili Ravi	0.9507	0.9279	0.9544	0.9456	0.9748	0.9577	0.9642	0.0978
CB Cattle	0.9276	0.9664	0.9497	0.8901	0.9742	0.9516	0.9638	0.4261

Figure 4.26: Performance Comparison of six Machine Learning Models and two Conventional Lactation Curve models across different dairy animals using STDMY

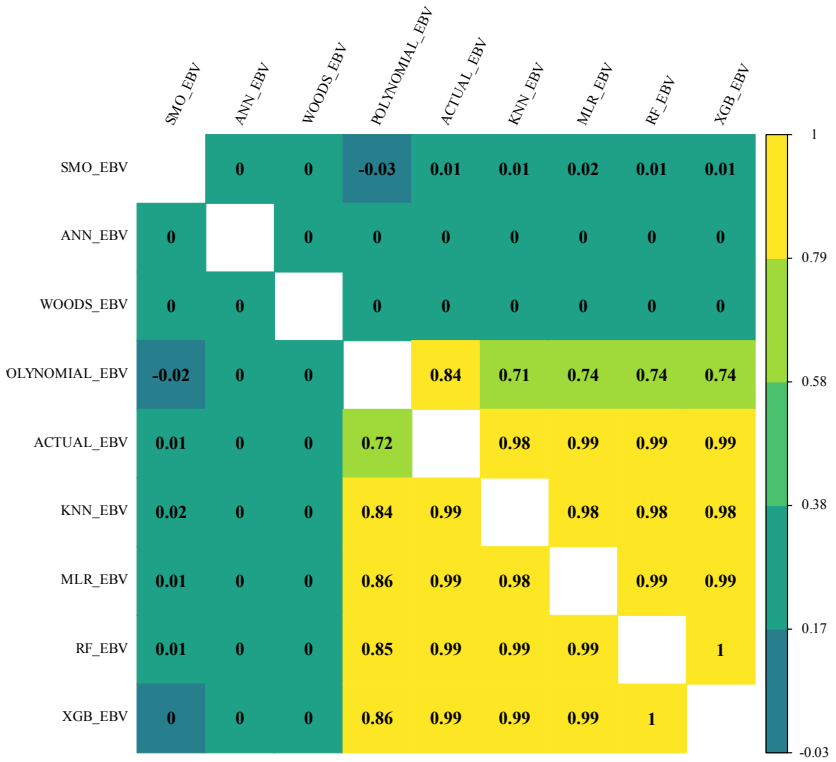

Figure 4.27: Heatmap of Pearson's (above diagonal) and Spearman's (below diagonal) correlation coefficients of EBV among the models for Murrah buffaloes

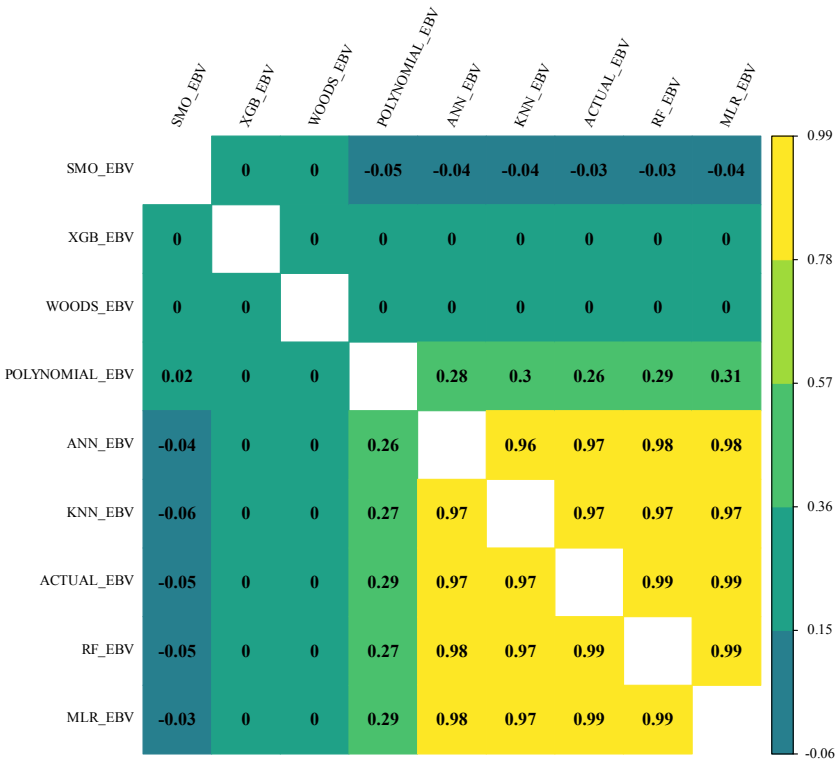

Figure 4.28: Heatmap of Pearson's (above diagonal) and Spearman's (below diagonal) correlation coefficients of EBV among the models for Nili Ravi buffaloes

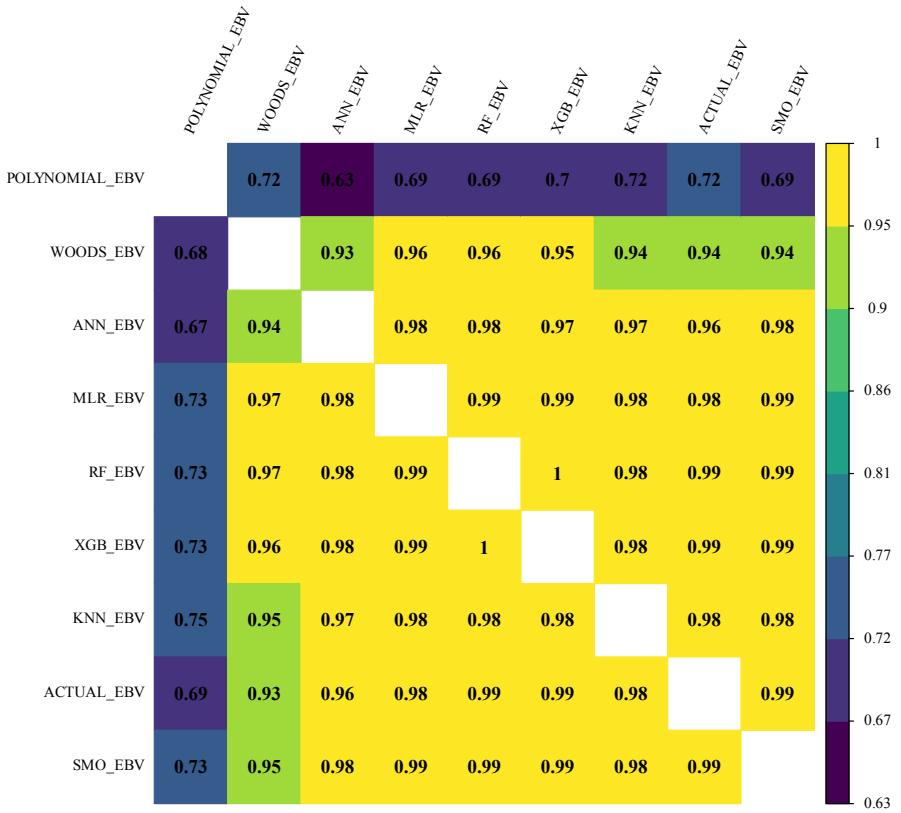

Figure 4.29: Heatmap of Pearson's (above diagonal) and Spearman's (below diagonal) correlation coefficients of EBV among the models for crossbred cattle

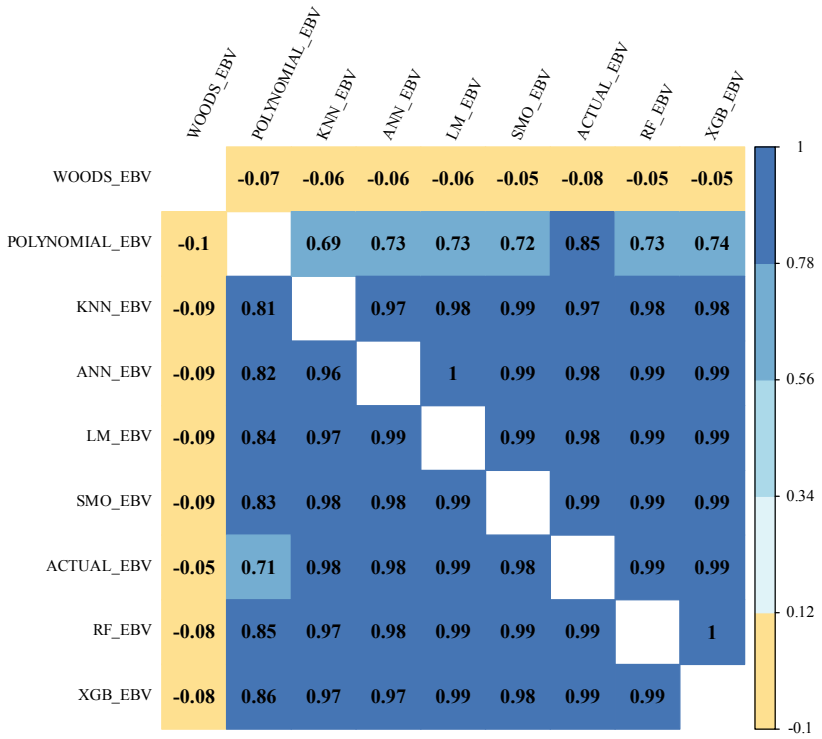

Figure 4.30: Heatmap of Pearson's (above diagonal) and Spearman's (below diagonal) correlation coefficients of sire evaluation among the models for Murrah buffaloes

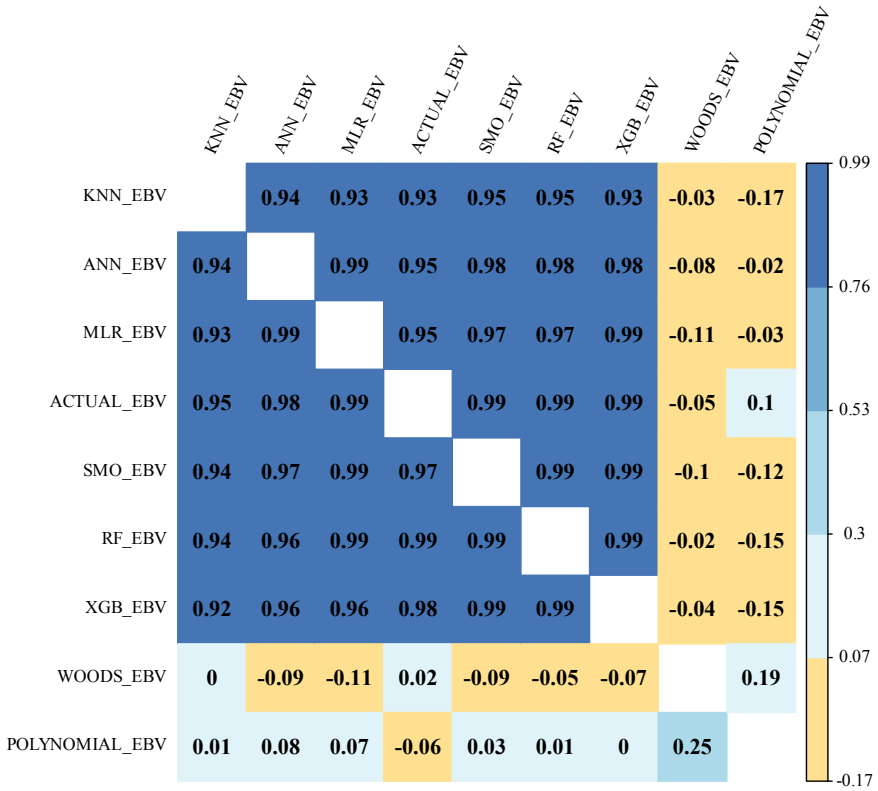

Figure 4.31: Heatmap of Pearson's (above diagonal) and Spearman's (below diagonal) correlation coefficients of sire evaluation among the models for Nili Ravi buffaloes

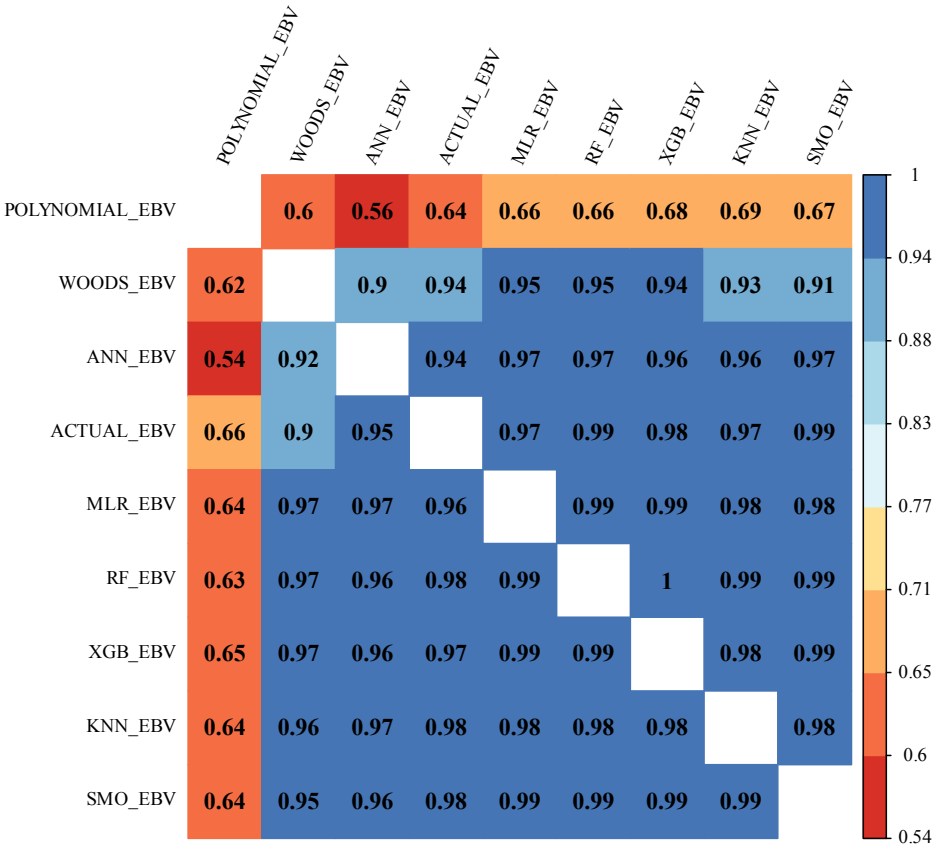

Figure 4.32: Heatmap of Pearson's (above diagonal) and Spearman's (below diagonal) correlation coefficients of sire evaluation among the models for crossbred cattle